Title

Dopamine modulation of spike dynamics in bursting neurons

Journal

European Journal of Neuroscience, 21(3)

ISSN

0953-816X

Authors

Szücs, Attila
Abarbanel, HDI
Rabinovich, M I
et al.

Publication Date

2005-02-01

Peer reviewed

European Journal of Neuroscience, Vol. 21, pp. 763–772, 2005

Dopamine modulation of spike dynamics in bursting neurons

Attila Szücs,[1,3] Henry D. I. Abarbanel,[1,2] Michail I. Rabinovich[1] and Allen I. Selverston[1]
[1]Institute for Nonlinear Science, University of California San Diego, 9500 Gilman Drive, La Jolla, CA 92093–0402, USA
[2]Department of Physics and Marine Physical Laboratory, Scripps Institution of Oceanography; University of California San Diego, La Jolla, CA 92093–0402, USA
[3]Balaton Limnological Research Institute of the Hungarian Academy of Sciences, Tihany, Hungary H-8237

Keywords: interspike interval, oscillation, pattern, signature, stomatogastric ganglion

Abstract

The pyloric network of the lobster stomatogastric ganglion is a prime example of an oscillatory neural circuit. In our previous study on the firing patterns of pyloric neurons we observed characteristic temporal structures termed 'interspike interval (ISI) signatures' which were found to depend on the synaptic connectivity of the network. Dopamine, a well-known modulator of the pyloric network, is known to affect inhibitory synapses so it might also tune the fine temporal structure of intraburst spikes, a phenomenon not previously investigated. In the recent work we study the DA modulation of ISI patterns of two identified pyloric neurons in normal conditions and after blocking their glutamatergic synaptic connections. Dopamine (10–50 μM) strongly regularizes the firing of the lateral pyloric (LP) and pyloric dilator (PD) neurons by increasing the reliability of recurrent spike patterns. The most dramatic effect is observed in the LP, where precisely replicated spike multiplets appear in a normally 'noisy' neuron. The DA-induced regularization of intraburst spike patterns requires functional glutamatergic inputs to the LP neuron and this effect cannot be mimicked by simple intracellular depolarization. Inhibitory synaptic inputs arriving before the bursts are important factors in shaping the intraburst spike dynamics of both the PD and the LP neurons. Our data reveal a novel aspect of chemical neuromodulation in oscillatory neural networks. This effect sets in at concentrations lower than those affecting the overall burst pattern of the network. The sensitivity of intraburst spike dynamics to preceding synaptic inputs also suggests a novel method of temporal coding in neural bursters.

Introduction

The stomatogastric ganglion (STG) of crustaceans contains several compact circuits of oscillatory neurons known as central pattern generators (CPGs). These networks and particularly the pyloric CPG have been prime experimental models of neuromodulation (Harris-Warrick *et al*., 1992). Although the synaptic connectivity of the neural circuit and the underlying neurochemical mechanisms are relatively simple, the system is capable of producing a wide variety of activity patterns and displays remarkable flexibility. Neuromodulators including monoamines are central players in the dynamic regulation of the neural network (Harris-Warrick *et al*., 1998). While monoamines are not produced by neurons within the STG, these substances can reach the pyloric neurons via the stomatogastric nerve which is the main pathway of modulatory inputs to the pyloric network. The biophysical mechanisms underlying the actions of monoamines have been well documented in the pyloric system (Johnson *et al*., 1993; Kloppenburg *et al*., 1999; Peck *et al*., 2001; Johnson *et al*., 2003). By adjusting the amplitude and timing of burst oscillations, monoamines exert characteristic changes in the operation of the pyloric network. Indeed, the modulation of voltage output of pyloric neurons by monoamines has received much attention. Because the timing of bursts and the number of spikes in bursts are among the most important determinants of the motor output (Morris & Hooper, 1997) and these parameters are effectively modulated by monoamines, virtually all earlier studies focused on the effects on these gross parameters of pyloric activity.

Results from our laboratory, however, showed that the fine structure of burst and spike patterns is subject to synaptic modulation in the pyloric CPG (Szücs *et al*., 2003). The synaptic connectivity of the network and the activity level of presynaptic neurons have a strong impact on the spike dynamics of the postsynaptic neurons. The changes in the regularity of spike timing by synaptic factors have been demonstrated by analysing the serial dependence of interspike intervals (ISIs). We identified cell-specific and characteristic ISI patterns within the bursts, referred to as ISI signatures of the neurons. Considering the known synaptic effects of neuromodulators on the pyloric network we can also expect the modulation of spike timing and ISI signatures of the component neurons.

Bursts are not limited to motor pattern generating neurons only. Recent experiments and theoretical studies have been accumulating evidence for the idea that the spike timing within bursts is regulated in such a way as to provide efficient and reliable information transmission between neurons (Fanselow *et al*., 2001; Balasubramanian & Berry, 2002; Derjean *et al*., 2003). Neuromodulators, while demonstrably affecting the overall activity of oscillatory neural networks (Ruskin *et al*., 1999; Svensson *et al*., 2003), probably play an important role in the regulation of the envelope and temporal structure of bursts, too.

This latter aspect of chemical neuromodulation is the subject of the current work. We analyse the modulation of intraburst spike dynamics of selected pyloric neurons by dopamine (DA), a potent

Correspondence: Dr Attila Szücs, [1]Institute for Nonlinear Science, as above.
E-mail: aszucs@ucsd.edu

Received 22 July 2004, revised 12 November 2004, accepted 18 November 2004

doi:10.1111/j.1460-9568.2005.03894.x

neuromodulator of the pyloric system. We show that this monoamine exerts robust and cell-specific effects on the spike dynamics of the neurons.

Materials and methods

Animals

Panulirus interruptus were obtained from Don Tomlinson Commercial Fishing (San Diego, CA, USA). The animals were kept in aerated seawater at 15–16 °C. Prior to dissection the animals were cold-anaesthetized by packing them in ice for 30–40 min.

Solutions

In experiments involving normal circuitry of the pyloric CPG we used the standard *Panulirus* physiological saline composed of (in mM) NaCl, 483; KCl, 12.7; $CaCl_2$, 13.7; $MgSO_4$, 10; $NaSO_4$, 4; HEPES, 5; and TES, 5; pH was set to 7.40. Partial isolation of the pyloric neurons was achieved with picrotoxin (PTX; 8 μM). PTX effectively blocked fast glutamatergic synapses (Bidaut, 1980; Marder & Eisen, 1984) while not affecting cholinergic connections. DA (Sigma) was dissolved in distilled water and kept frozen in stock solutions (10^{-2} M). DA (10–50 μM final concentration) was bath-applied using a continuous microperfusion at a rate of 2–3 mL/min.

Preparation

The complete stomatogastric nervous system containing the STG and the anterior commissural and esophageal ganglia was separated from the stomach (Mulloney & Selverston, 1974) and pinned in a silicone elastomer (Silgard 184, Dow Corning, Midland, MI, USA)-lined Petri dish. Interconnecting nerves as well as the output motor nerves of the STG were left intact. The connective sheath of the STG was removed using sharp forceps to facilitate access to the somata of the neurons. The STG was enclosed in a small well of petroleum jelly that served as a separate perfusion chamber of ≈2 mL volume. DA was applied in the STG chamber while the anterior ganglia were bathed in normal physiological saline. Care was taken to maintain a stable and smooth flow in the perfusion chamber. The temperature of the preparation was held at 16–18 °C using a thermoelectric Peltier cooler attached to the bottom surface of the preparation dish.

Electrophysiology

Intracellular recordings were made using Neuroprobe 1600 bridge amplifiers (A-M Systems Inc., Carlsborg, WA, USA). Microelectrodes were filled with 3 M K-acetate plus 0.1 M KCl solution and had a resistance of 12–15 MΩ. Cell identification was achieved by comparing intracellular membrane potential traces with simultaneous extracellular recordings from nerves leaving the STG. Extracellular signals were measured using an A-M 1700 differential AC amplifier (A-M Systems).

Data acquisition

Voltage traces of the pyloric neurons (Fig. 1A) were acquired at 20 kHz by a computer equipped by a PCI-MIO-16E4 data acquisition board (National Instruments, Austin, TX, USA) and running the DASYLab 5.6 program (Datalog GmbH, Germany). Action potential (spike) occurrences were detected in real time by calculating the first time-derivative of the intracellular membrane potential and observing its local maxima. The arrival times of spikes of each recorded neuron were saved sequentially in separate ASCII files. The error in measurement of spike times was 0.05 ms. Care was taken to monitor the reliability of the spike detection. We excluded data from the analysis acquired during transient disruptions of the pyloric oscillation by cardiac sac episodes. Control firing patterns (before application), DA-modulated patterns and the washout were all recorded in the same files, each epoch lasting 200–400 s. The typical length of the spike trains was 1000 s per experiment (DA application), each file containing at least 1000 bursts per neuron.

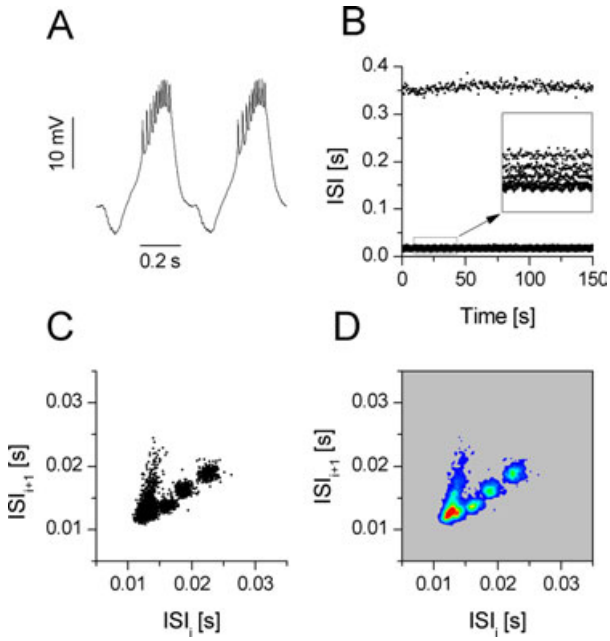

FIG. 1. Characterization of the spike timing and serial dependence of ISIs in a bursting pyloric neuron. (A) Two bursts in the membrane voltage waveform of the PD neuron. (B) The sequential ISI plot obtained from the spike times of the same neuron. The insert shows the population of intraburst ISIs. (C) The return map constructed from the short ISIs (long ISIs are not displayed). (D) Density plot of the return map (joint ISI probability distribution) in a grayscale-coded form (colour-coded on line).

Data analysis

Detailed quantitative analysis was performed using the spike trains $\{t_i\} = \{t_1, t_2, t_3 \ldots t_N\}$, where $t_1 < t_2 < t_3 \ldots$ are successive spike arrival times available for each neuron recorded. Timing of the spikes relative to the preceding one was characterized by the interspike interval (ISI, first-order): $ISI_i = t_{i+1} - t_i$. ISI sequential graphs were constructed by plotting interspike intervals ISI_i as a function of the elapsed time (Fig. 1B). Relations between successive ISIs were graphically demonstrated by ISI return maps, also called joint interspike interval plots or Poincaré maps (Dekhuijzen & Bagust, 1996; Segundo *et al.*, 1998; Fitzurka & Tam, 1999; Faure *et al.*, 2000). Here, ISI_{i+1} was scatter-plotted against ISI_i for each $i \leq N - 2$ (Fig. 1C). Consequently, points in these plots correspond to pairs of consecutive ISIs among three adjacent spikes. The return maps typically contain thousands of points forming an attractor. We have earlier shown that the shape of such attractors is cell-specific and it also reflects the synaptic inputs received by the neuron (Szücs *et al.*, 2003). To characterize the local density of the return maps we calculated joint-interval probability density histograms using a two-variable Gaussian kernel (Parzen estimation; Sanderson & Kobler,

1976; Szücs *et al*., 2003). These histograms appear in the figures in a gray-scale-coded form (colour coded on line) (Fig. 1D). Areas with warmer colours (toward red) indicate higher local density of points. These histograms appear in the figures in a grayscale-coded form (Fig. 1D). Gradually darker areas (or gradually warmer colours) indicate higher local density of points. Zero-density areas are coloured as a light-grey background for better visualization and separation of the nonempty areas.

As a general rule, ISI graphs of periodically bursting neurons display two main populations. Short ISIs (< 0.1 s for most pyloric neurons) correspond to the spike events within bursts while long ISIs (> 0.2 s) separate the last spike of the recent burst from the first spike of the following one (Fig. 1B). In the paper we focus on the analysis of spike patterns within bursts (intraburst ISIs). Moreover, ISI return maps of such neurons contain three clusters of points, with the intraburst ISIs located in the cluster closest to the origin of the graph. We display only the intraburst clusters in the figures, so the other two clusters corresponding to interburst intervals are omitted.

Results

DA is well known as an effective modulator of the voltage output and the overall burst pattern of pyloric neurons (Flamm & Harris-Warrick, 1986a; Ayali & Harris-Warrick, 1999). DA and other monoamines exert differential and cell type-dependent effects. Importantly, monoamines not only change the intrinsic membrane properties of the neurons but they also act on the synaptic connections among them (Harris-Warrick *et al*., 1998). Therefore, DA-induced modulation of intraburst spike dynamics, if observed, can be a consequence of modulation on several targets. However, pharmacological manipulation of synaptic connectivity prior to DA application can be used to distinguish between different types of modulatory action. In the present study we describe DA modulation of spike patterns in two neurons of the circuit from a total of 16 preparations. The lateral pyloric (LP) and the pyloric dilator (PD) neurons are important components of the network. There are two electrically coupled PDs and together with the anterior burster (AB) neuron they form the pacemaker group. The LP and PD neurons, when normally bursting in the intact circuit, mutually inhibit each other through glutamatergic (LP) and cholinergic (PD) synapses.

DA effects on the burst temporal parameters of pyloric neurons

Figure 2 demonstrates the modulatory effect of DA (20 μM) on these neurons. DA exerted differential effects on these cells: the LP was depolarized and the onset of the bursts became steeper (Fig. 2A) while the opposite was seen in the PD neuron (Fig. 2B). At the same time, we observed characteristic changes in the number and temporal distribution of the intraburst spikes, too. Local spike frequency (f_{sp}), defined as the number of spikes in bursts divided by the burst duration, showed marked changes during DA application. The LP neuron fired more rapidly during the bursts (Fig. 2D) while the PD displayed the opposite behaviour (Fig. 2E). The changes in the local firing rate of the cells appeared more significant than those in the overall burst parameters. When plotting the instantaneous burst frequency (f_b), defined as the reciprocal of the burst cycle period against the elapsed time, we found only a slight increase during DA application (Fig. 2C). Commonly, the neurons displayed more dramatic changes in the parameters of their intraburst dynamics than in the parameters of the overall bursting pattern (10–50 μM concentrations). We noted that marked changes in the overall burst parameters could be expected at

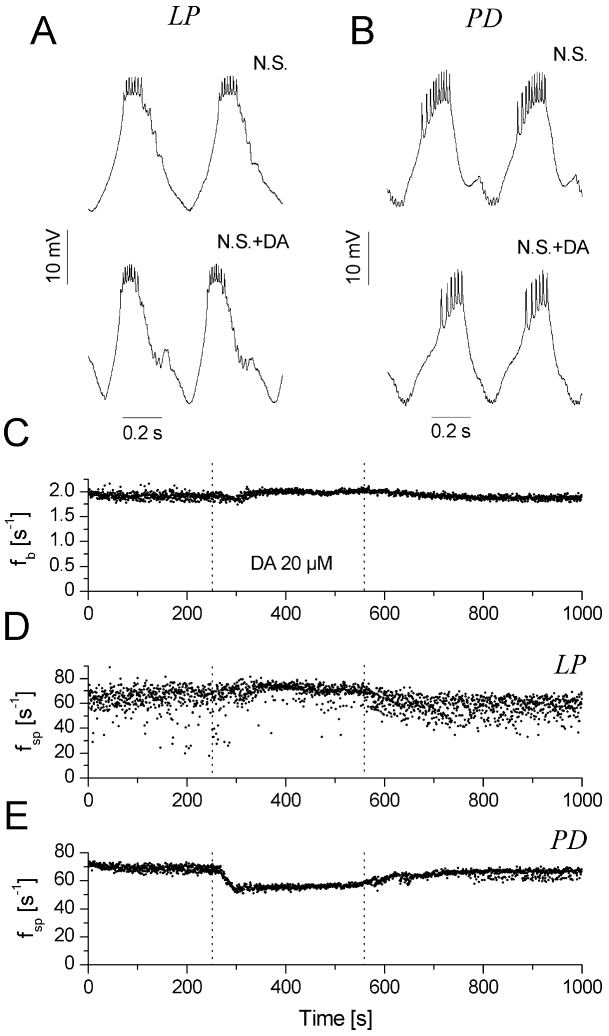

FIG. 2. DA alters both the membrane potential waveform and the burst temporal parameters of pyloric neurons. Burst oscillations of (A) the LP and (B) the PD neurons are compared in control and during the application of 20 μM DA (N.S., normal saline). DA clearly alters the voltage slope especially at the onset phase of the burst oscillations. (C) Frequency of the pyloric oscillation (reciprocal of the burst cycle period of the PD neuron) as a function of the elapsed time during the entire experiment (1000 s). (D and E) Local spike frequency f_{sp} of the LP and PD neurons, respectively. The local spike frequency of the LP neuron slightly increased and displayed smaller variations during the application of DA. The application began at t = 270 s followed by washout at t = 560 s. The effect was reversible in both neurons.

100 μM and higher concentrations, as demonstrated in earlier studies (Flamm & Harris-Warrick, 1986a; Ayali & Harris-Warrick, 1999).

To address the role of fast inhibitory synaptic connections in the DA-induced modulation of intraburst spike patterns we used a reduced configuration of the pyloric neurons. Picrotoxin (PTX) is an effective blocker of glutamatergic neurotransmission in the stomatogastric nervous system (Marder & Eisen, 1984). Typically, PTX removed fast inhibitory postsynaptic potentials (IPSPs) from the voltage traces of the neurons, hence their oscillations became smoother (Fig. 3A and B). In a normal circuit with full connectivity the LP neuron receives multiple phasic synaptic inputs during its burst oscillations but the IPSPs disappeared when the PTX saline was applied. The PD neuron, on the other hand, received only one phasic inhibitory input, the one from the LP neuron. This inhibition, being a glutamatergic one, could be blocked with PTX. The action of DA seen in normal saline was

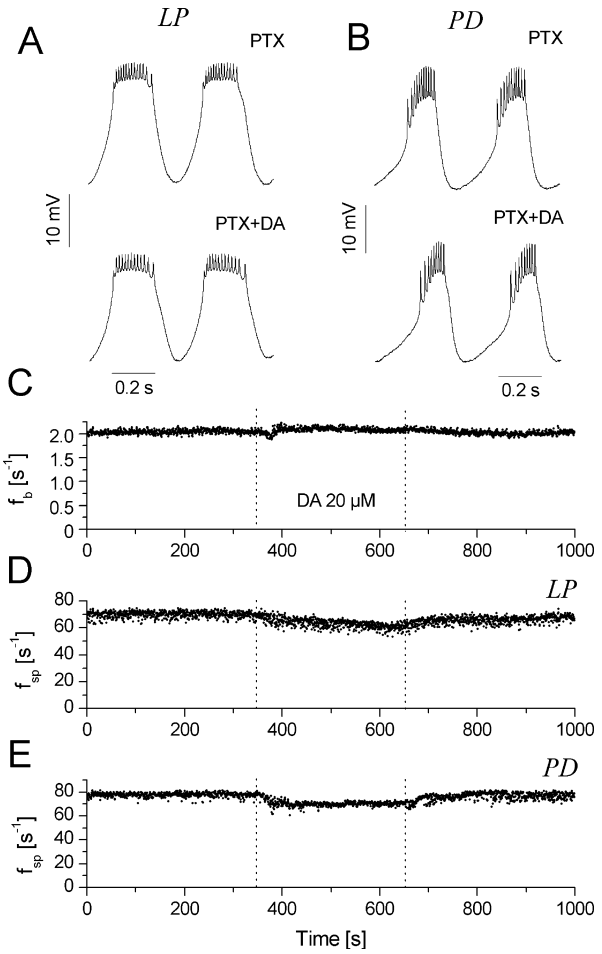

FIG. 3. DA effects on (A) the LP and (B) the PD neurons with their glutamatergic inputs blocked. The preparation was held in PTX-containing saline but inputs from anterior centres were left intact. DA (20 μM) exerted relatively weak effects on the voltage output and burst temporal parameters of the two neurons when compared to Fig. 2. (C) The burst frequency of the pyloric rhythm was barely changed during the DA application. (D and E) Both neurons displayed a weak decrease in their local spike frequency. The effect on the LP neuron's spike frequency was markedly different form that seen in normal saline (Fig. 2D).

greatly reduced when using a PTX-containing solution (of the same DA concentration). While the general depolarizing effect on the LP neuron and the hyperpolarization of the PD neuron was still identifiable, the voltage waveforms during DA application were remarkably similar to the control ones. The local spike frequency of the LP and PD neurons (Fig. 3D and E) was less affected by DA than in the normal saline and the overall burst frequency of the pyloric rhythm was virtually unchanged (Fig. 3C). These observations suggest that DA exerts its effect on the temporal parameters of firing patterns at least in part by acting through glutamatergic synaptic connections. Once the glutamatergic connections were blocked, and could not be modulated by DA, the effects were somewhat reduced. These finding are further supported by our data on the ISI structures described below.

DA modulated the ISI signatures of pyloric neurons

The sequential plots of ISIs of pyloric neurons typically display two main populations, those of ISIs within bursts (< 0.05 s) and those between bursts (> 0.2 s). Hence, onsets of burst could be easily detected by finding episodes when a long ISI is followed by a short one. The distinction between intraburst and interburst ISIs is straightforward when the neurons display a stable oscillatory pattern, i.e. transient extrinsic synaptic inputs such as cardiac sac episodes are not present. Cardiac sac episodes temporally disrupt the pyloric rhythm and induce irregular firing in the neurons (Ayali & Harris-Warrick, 1998). Therefore, cell-specific ISI patterns (signatures) can be observed only in pyloric neurons with stable bursting and receiving no interfering synaptic inputs (Szücs *et al.*, 2003). We also note that stable bursting requires intact descending modulatory inputs from anterior centres, hence sucrose block on the stomatogastric nerve (Flamm & Harris-Warrick, 1986a) was not used in any of the experiments.

DA induced characteristic changes in the temporal patterns of intraburst spikes in the two types of pyloric neurons we used. ISI sequences recorded during the application show gradual changes as the modulatory effect of DA developed (Fig. 4A). In control conditions the LP neuron produced a firing pattern with a typical comet-like ISI return map (Fig. 4B). The attractor occupied the upper left half of the map relative to the diagonal indicating the continuous increase of ISI durations as the burst developed. In such conditions the LP neuron behaved as an irregular (noisy) burster with low reproducibility of bursts. Remarkably, in the presence of DA the comet-like cluster collapsed into very compact and separated densities (Fig. 4C). The regularity of spike timing in successive bursts increased dramatically: dispersion (jitter) of the intraburst ISIs dropped (Fig. 5). DA exerted a very specific and robust effect on the LP neuron: it made it a regular and precise burster with very low spike jitter in the successive bursts. The DA-induced regularization of the LP neuron was highly reproducible and observed in 12 different preparations. The effect was so robust and characteristic that the emerging ISI pattern clearly identified the LP neuron under DA modulation; it could be called the DA signature of the LP neuron.

DA, while exerting a hyperpolarizing effect on the PD neuron, also affected its intraburst spike dynamics. The *V*-shaped return map with slightly overlapping clusters (a typical PD signature) was observed under control conditions (Fig. 4E). Here, separated clusters indicate recurrent spike patterns in the successive bursts of the PD neuron. Another distinctive feature of the PD signature was that the clusters were located below the diagonal of the return map corresponding to gradually decreasing ISI durations. DA not only shifted the point clusters (ISIs prolonged) but also clearly separated them (Fig. 4F). Four compact clusters are present, indicating very reliable repetition of ISIs and small jitter in spike arrival times. Hence, DA modulated the spike dynamics of the PD neuron and induced more reliable and precise repetition of bursts, an effect similar to that in the LP neuron. This regularizing effect was observed in 16 preparations.

As we noted above, DA exerts differential effects on the pyloric neurons: some of them are depolarized, others inhibited. Bursts of the LP neuron became more compact and intense during DA application while the PD responded the other way. Nevertheless, the dispersion of intraburst spikes was markedly decreased in both the excited (LP, Fig. 5A) and inhibited (PD, Fig. 5B) neurons. Another notable aspect of the DA-induced regularizing effect is that it set in at a lower concentration (below 10 μM for the LP) than that affecting the overall burst frequency or burst phases. Evaluating data from several preparations showed that the mean burst frequency of the overall motor pattern increased only by 8.9 ± 12.6% ($n = 12$) when using 20 μM DA and by 14.1 ± 10.7% ($n = 11$) when using 50 μM DA (both relative increments ± SD; see also Table 1 for absolute values). These can be considered weak effects compared to those observed in the intraburst spike patterns.

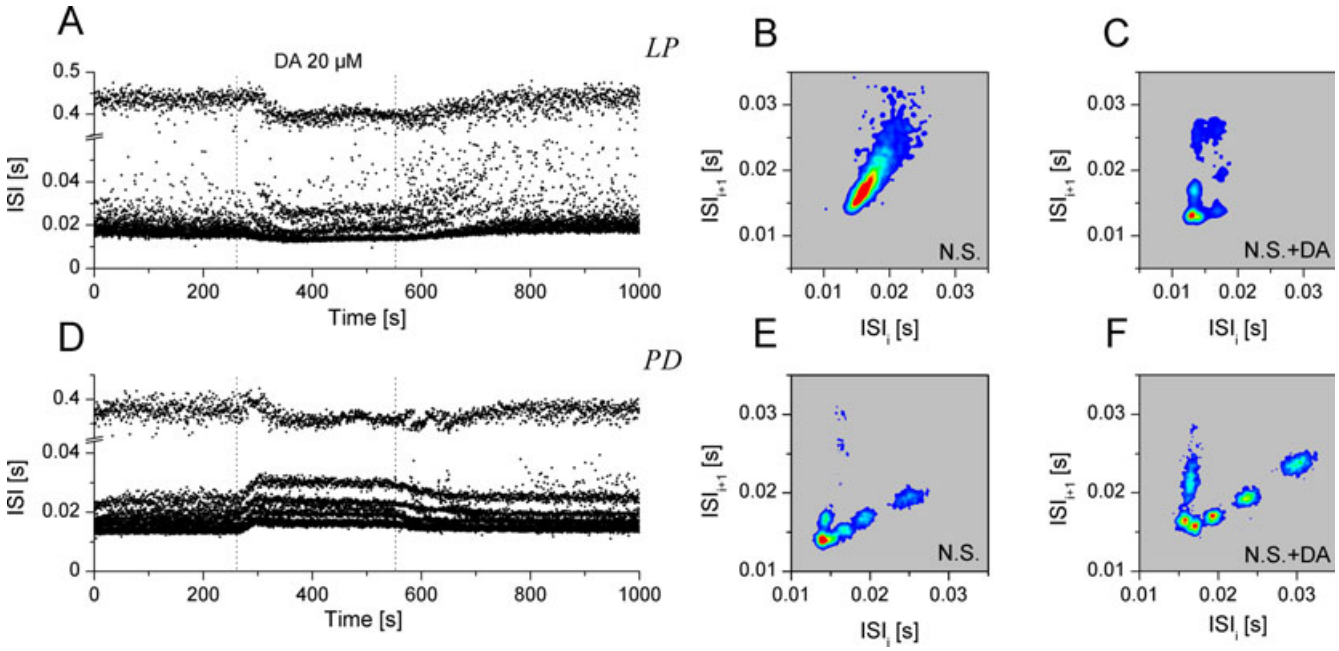

FIG. 4. DA effectively modulates the intraburst firing patterns of pyloric neurons. (A and D) Sequential plots of the ISIs in the LP and PD neurons, respectively. Note the well separated populations of short (intraburst) and long (interburst) ISIs. DA (20 μM) exerted differential effects in the neurons: average intraburst ISIs of the LP were decreased while those of the PD were increased. Note the banding of points during the application of DA. Density plots of the ISI return maps are compared for the two neurons (B and E) before and (C and F) during the application of DA. The breakup of the attractors and emergence of compact separated clusters can be observed. The frequency of pyloric bursting was 1.92 ± 0.06 and 2.00 ± 0.03 Hz before and during DA application, respectively.

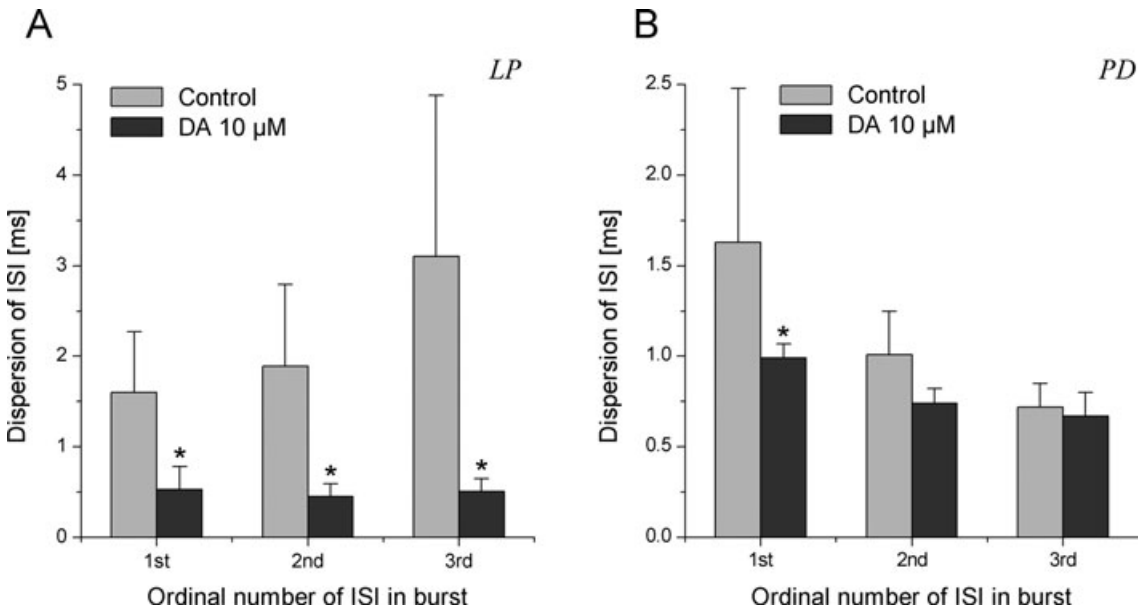

FIG. 5. DA dramatically decreases the disperison (SD) of ISIs in the pyloric neurons. ISIs between the first second and third pairs of spikes within the bursts of (A) the LP and (B) the PD neurons (both $n = 6$) were compared in control and during DA application (10 μM). The SD of the ISIs dropped in both neurons especially in the LP. Note the tendency in control conditions for the spike jitter of the LP to become greater with increasing ISI number but the opposite to occur under the action of DA. *$P < 0.05$.

DA was less effective in a reduced configuration of the pyloric neurons

Because DA alters both intrinsic membrane conductances (Harris-Warrick *et al*., 1998; Kloppenburg *et al*., 1999) and synaptic connections (Harris-Warrick *et al*., 1992; Johnson & Harris-Warrick, 1997; Peck *et al*., 2001), the observed effect on the ISIs could be a consequence of modulatory actions on both types of targets. To estimate how the two kinds of modulation contribute to the observed changes in the ISI signatures, we used a reduced configuration of the pyloric network (using PTX). In PTX saline fast glutamatergic synapses are not functional, hence DA modulation of such inputs can

TABLE 1. Parameters of the firing patterns of the LP and PD neurons in normal conditions and under the modulatory action of DA

DA concentration	Normal saline				PTX saline			
	f_b (Hz)	$N_{sp,\ LP}$	$N_{sp,\ PD}$	n	f_b (Hz)	$N_{sp,\ LP}$	$N_{sp,\ PD}$	n
DA (0 μM)	1.88 ± 0.2	5.2 ± 1.4	9.9 ± 1.5	25	1.89 ± 0.15	8.1 ± 2.3	10.6 ± 2.4	13
DA (10 μM)	2.12 ± 0.35	6.1 ± 0.2	7.8 ± 1.4	4	1.91 ± 0.10	8.9 ± 3.4	8.9 ± 1.3	3
DA (20 μM)	2.03 ± 0.37*	6.6 ± 1.6*	6.1 ± 1.4$^{\#}$	12	1.99 ± 0.19	10.4 ± 2.6	6.4 ± 1.7$^{\#}$	7
DA (50 μM)	2.15 ± 0.32*	7.6 ± 2.0*	4.5 ± 2.2$^{\#}$	9	1.96 ± 0.40	10.1 ± 2.7	5.4 ± 2.4*	3

'Normal saline' and 'PTX saline' in the headings correspond to the two network configurations used in our study (full connectivity vs. blocked glutamatergic connections). Abbreviations are as follows: f_b, frequency of the pyloric oscillation; $N_{sp,\ LP}$ and $N_{sp,\ PD}$, number of spikes per burst for the LP and PD neurons, respectively; n, number of experiments. Values are given as mean ± SD $^*P < 0.05$, $^{\#}P < 0.005$, Student's t-test for paired data, 0-μM data as controls.

be ruled out. However, voltage-gated membrane conductances (e.g. transient or sustained K-currents; Kloppenburg *et al.*, 1999) of the individual cells as well as nonglutamatergic synaptic connections are still affected by DA, similar to that seen in normal conditions.

The effect of DA on the ISI patterns was found to be much weaker in PTX solution than under normal conditions. In striking contrast to the effect seen in normal saline, we find no regularization or reshaping of the ISI signature of the LP neuron when its glutamatergic synapses were blocked ($n = 6$). The return map of the LP is virtually indistinguishable before (Fig. 6B) and during (Fig. 6C) the application of DA. Dense and separated clusters, signs of precisely replicated ISI patterns, are not observed in the return maps; rather we see slanted and diffuse comet-like shapes. This is an indication of DA being ineffective in changing the dynamics of intraburst spiking of the LP neuron when glutamatergic connections were blocked. The PD neuron, when its glutamatergic input from the LP was blocked, displayed an ISI signature somewhat more compact and less clustered than that in normal conditions (compare Figs 6E and 3E). Hence, PTX itself changed the spike dynamics of the PD neuron (Szücs *et al.*, 2003). At the same time, when observing the ISI return map of the PD in PTX saline and during DA application, we found clearly separated clusters and the characteristic V shape (Fig. 6F). DA induced slight changes in the position of the clusters, and the typical PD signature (like that in normal saline) became more distinct. As a result, the effect of DA was similar to that observed in normal saline. As for the burst temporal parameters, DA in PTX saline exerted a minor effect: the relative increase in the mean burst frequency was 5.0 ± 7.7% ($n = 7$) with 20 μM DA and 5.4 ± 11.9% ($n = 3$) when using 50 μM DA.

Simulating the effect of DA with current injection

DA is a modulator of both intrinsic membrane properties such as voltage-gated ionic channels and the synaptic connections between the neurons. Each of the multiple target-specific actions of DA might, to some degree, contribute to the observed effects on the voltage output and spike dynamics of the cells. It is therefore very difficult to simulate experimentally the DA effect. Nevertheless, the general depolarizing and hyperpolarizing action of DA can be crudely

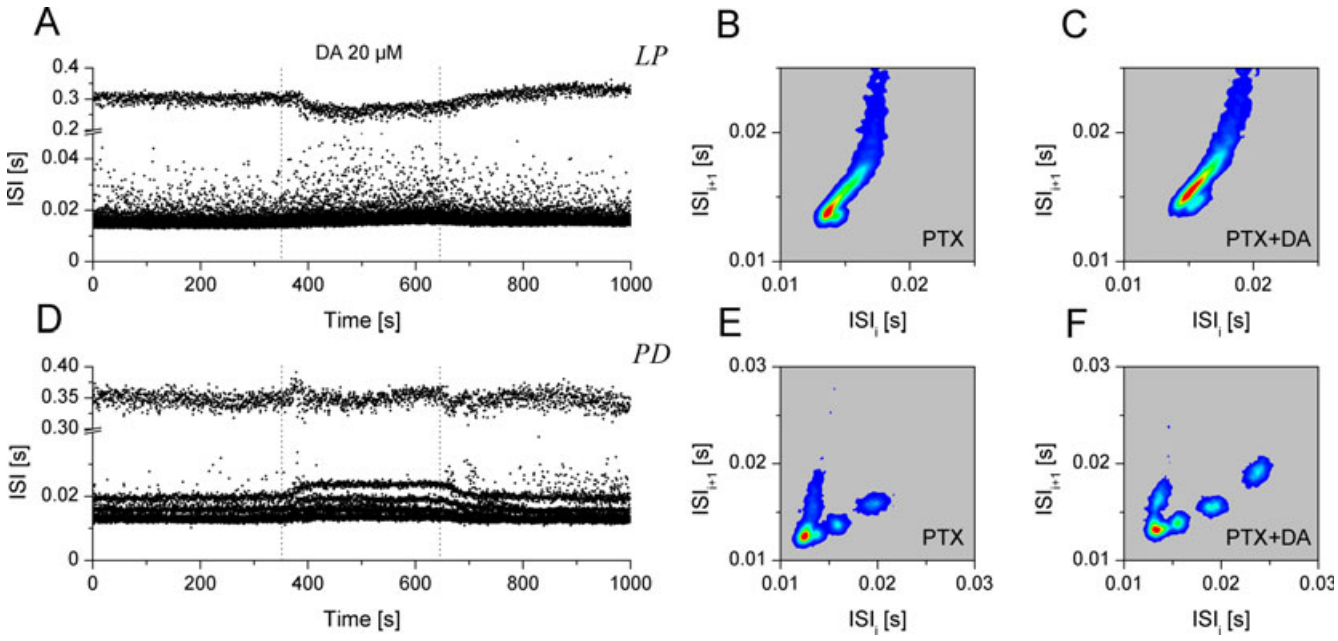

FIG. 6. DA is a less effective modulator of spike timing when applied in picrotoxin-containing saline. (A and D) Sequential plots of ISIs. (B and E) Return map density plots show the serial dependence of ISIs when only PTX was present (as control). (C and F) The corresponding graphs during DA (20 μM). Changes in the attractors are less apparent than those in Fig. 4. The intraburst spike dynamics of the LP was barely modulated by DA (C vs. B). The reshaping of the PD signature, however, was similar to that observed in normal saline (see Fig. 4). The pyloric bursting frequency was 2.04 ± 0.04 Hz before and 2.09 +0.04 Hz during DA application.

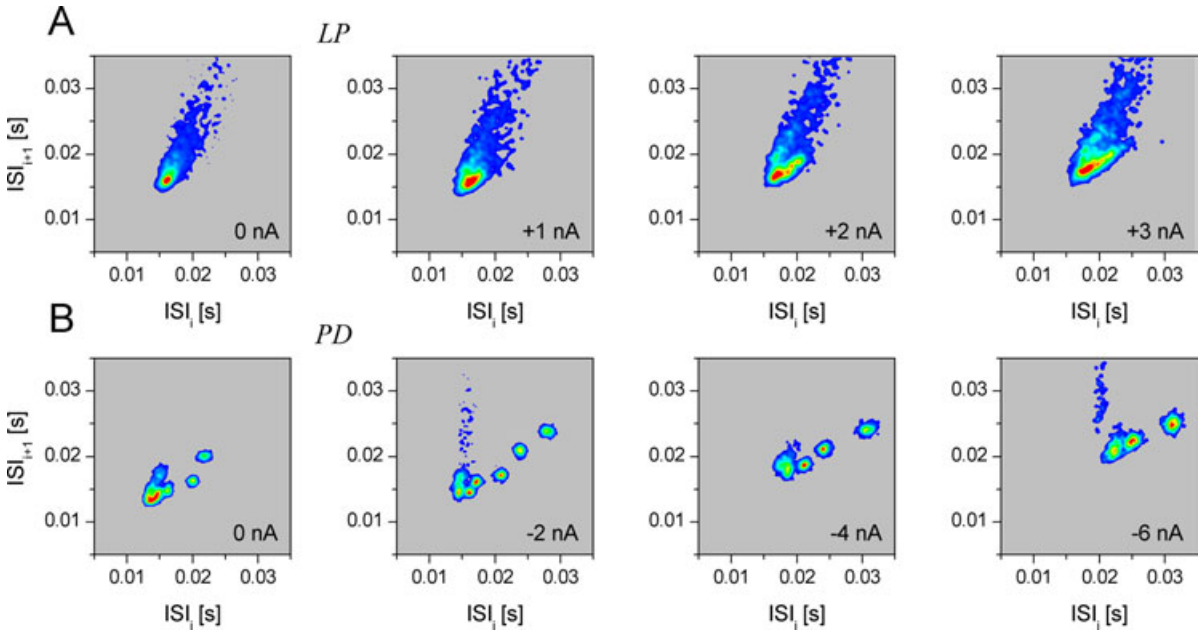

FIG. 7. Effect of intracellular current injections on the ISI signatures of bursting pyloric neurons. (A) Panels in the top row show the effect of the injected depolarizing current on the LP neuron. Gradually increasing levels of current resulted in a slight shift of the attractor toward longer ISI values but its overall appearance is similar to that in control conditions (I = 0 nA, left panel). (B) The bottom row shows the effect of hyperpolarizing current injection on the PD neuron. Here we observe clear clustering and the shape of the attractor strongly depends on the amount of injected current. The data were collected from two different preparations. In the experiment shown in (B) the pyloric oscillation was exceptionally periodic and stable.

mimicked by intracellular current injection. We used gradually increasing or decreasing steps of DC current each lasting 100 s to depolarize the LP neuron and to hyperpolarize the PD neuron. Figure 7 shows the data from two such experiments. The ISI signature of the LP neuron displayed some changes with increasing levels of current. Nevertheless, the characteristic DA signature could not be reproduced by current injection. We observed important differences between the return maps of the LP neuron under DA and when depolarized with DC current injection; the joint ISI map of the LP was still fuzzy and comet-shaped when DC current was used (Fig. 7A) while it contained very compact and separated densities during DA application. Furthermore, the 'mass centres' of the return maps shifted in different directions. DA produced short and precisely replicating ISIs in the LP (densities shifted toward the origin of the map) while the depolarizing current injection elicited an opposite effect. This finding is somewhat unexpected because in most neurons a depolarizing current tends to increase the firing rate, i.e. decreasing the ISIs. We note that in experiments with negative current injection into the LP neuron (−0.5 to −3.0 nA) the mean ISIs were actually decreased, i.e. the local spike frequency became higher. At the same time the clustering of the return map, a characteristic feature of DA modulation, was never observed. Injection of a constant depolarizing current therefore failed to reproduce the effect of DA on the LP neuron in normal saline. As for the PD neuron, hyperpolarization by negative current injection worked better in reshaping its ISI signature toward that observed under DA. Remarkably, increasing levels of the constant hyperpolarizing current resulted in different ISI return maps and relocation of the clusters (Fig. 7B) but the overall shape of the attractor (the *V* form) was still specific for the PD neuron. Tight and well-separated clusters in the return maps indicate precise replication of ISIs during the bursts. As an example, dispersion (SD) of the ISIs corresponding to the tight clusters in the return map at −2 nA current level was <0.5 ms. Hence, DA-induced reshaping of the intraburst spike dynamics of the PD neuron could be well mimicked by intracellular current injection. Note that the clusters were shifted toward the upper right part of the return maps as the magnitude of hyperpolarizing current was increased, similarly to that with increasing concentration of DA.

Discussion

The data presented here demonstrate neurochemical modulation of spike patterns in the bursting neurons of the crustacean nervous system. While the effects of monoamines and peptides on the overall pyloric burst pattern have been extensively studied, chemical modulation of the intraburst spike dynamics has not yet been investigated. This type of neuromodulation is a novel phenomenon and there has been only one similar report describing the modulation of burst patterns in the locust frontal ganglion (Zilberstein *et al*., 2004).

The neuromodulator DA reshapes the fine structure of spike patterns while affecting the frequency of pyloric rhythm to a lesser degree. Picrotoxin, a potent blocker of the fast glutamatergic inhibitory neurotransmission, abolishes the modulatory effect of DA on the lateral pyloric neurons' firing pattern. At the same time, PTX has a weak effect on the DA-induced reshaping of the ISI signature of the PD neuron.

Possible biophysical mechanisms in the modulation of pyloric spike patterns

The effects of monoamines on the overall network activity (Flamm & Harris-Warrick, 1986a; Harris-Warrick *et al*., 1992; Johnson *et al*., 1995; Ayali *et al*., 1998; Ayali & Harris-Warrick, 1999) as well as the synaptic and intrinsic properties of the component neurons (Flamm & Harris-Warrick, 1986b; Johnson & Harris-Warrick, 1997; Kloppenburg *et al*., 1999; Peck *et al*., 2001) have been extensively studied. These studies have revealed a variety of motor output patterns for the pyloric network induced by various monoamines. Monoamines

are capable of reconfiguring the network output by altering voltage-gated conductances of the cells and, at the same time, tuning chemical synapses. In our experiments DA exerted novel effects, namely the modulation of spike dynamics within bursts, appearing especially strongly in the LP neuron. Here we observed the appearance of precisely replicating spike patterns in a normally 'noisy' neuron. It is important to say that there are several (usually two or three) tight clusters in the return maps of the LP neuron during DA application. A single density (a fixed point along the diagonal of the return map) would indicate the repetition of equal ISIs, like those appearing in a periodically spiking neuron. Considering the biophysically possible highest frequency firing (saturation) during the burst plateaus one would observe the replication of the shortest possible ISIs with a tight single cluster in the return map. As we see, the LP neuron produces spike dynamics far more complex than this kind of saturation during the action of DA. Multiple clusters during DA indicates a temporally structured but precisely repeating firing pattern. This is a very characteristic feature of DA modulation on the LP and similar clustering effects were not found to such a degree in other pyloric neurons.

In normal conditions the LP neuron receives potent synaptic signals before and during its burst plateau potential. The characteristic DA signature of the LP neuron is certainly related to these synaptic inputs because PTX block of glutamatergic connections abolishes the DA effect. Several glutamatergic inputs have been identified on the LP neuron. PY neurons are intrinsic components of the pyloric network and, being glutamatergic, they produce fast IPSPs in the LP neuron (Russell & Hartline, 1982). DA exerts a strong depolarizing effect the PY neurons (Flamm & Harris-Warrick, 1986a) so the IPSPs arriving from the PYs become more frequent. In addition to the PY neurons, the LP receives inputs from neurons extrinsic to the STG. P-cells have been described as important modulatory inputs to the pyloric network and they deliver potent phasic excitation to the LP neuron (Russell & Hartline, 1982). There is evidence that the P-cell in the *Homarus* is a GABAergic modulatory interneuron and its effect on the postsynaptic pyloric neurons, including the LP neuron, can be blocked by picrotoxin (Nagy *et al*., 1994); however, this requires higher concentration of PTX than used in our experiments.

To explain the dramatic DA-induced increase in spike timing regularity in the LP we inspected the neurons' voltage waveforms. In normal conditions the bursts of the LP are influenced by potent IPSPs arriving from the PY neurons. These IPSPs tend to arrive more frequently during the second half of the bursts, but a few can be detected even during the early phase. The IPSPs influence the generation of spikes, hence the regularity of spike timing is reduced. Therefore, the noisy and comet-shaped ISI signature of the LP (in normal saline) is a consequence of the frequent and irregular IPSPs from the PY neurons. Among the multiple effects of DA the shifting of the LP–PY burst phase plays a crucial role in regularizing the spike dynamics of the LP neuron. As reported earlier (Harris-Warrick *et al*., 1998) and also illustrated in Fig. 8, the IPSPs from the PY neuron appear later in the burst of the LP neuron when DA is present. Hence, the spike emissions of the LP neuron are not disrupted by the IPSPs from the PY neurons. This results in a more regular spiking. At the same time, the regularization of spike dynamics of the LP neuron cannot be explained by the shift of the LP–PY phase alone. Remember that such DA-induced regularization is not observed in PTX saline, when the IPSPs from the PYs are entirely absent. In normal conditions DA also enhances the activity of the AB neuron. The AB neuron delivers phasic inhibition to the LP and this action is enhanced by DA (Johnson *et al*., 1995; Harris-Warrick *et al*., 1998). Moreover, the AB–LP burst phase becomes shorter which makes the LP's

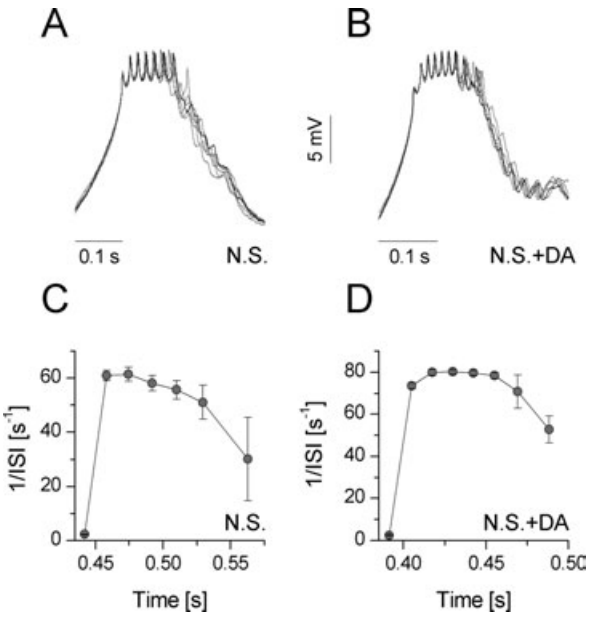

FIG. 8. The regularity of spike timing in the LP neuron strongly depends on the synaptic inputs and was modulated by DA. The top panels show six overlapping bursts in (A) control conditions and (B) during the application of 50 μM DA. In control conditions the late part of the burst displays 'noisy' voltage fluctuations (IPSPs) and jitter in spike timing (A). DA shifted the IPSP backward; thus the spike emissions during the early phase of the bursts become very regular. (C and D) The average instantaneous firing frequency (reciprocal of the ISIs) along the burst of the LP neuron in normal conditions and with DA, respectively. The values show greater SDs in control than during DA application. The number of successive bursts used to calculate the graphs was $n = 190$ (C) and $n = 147$ (D).

postinhibitory rebound steeper. The enhanced preburst inhibition by the AB neuron and the increased delay of the IPSPs from the PY neurons both contribute to the reshaping of the spike dynamics of the LP neuron. Note that PTX blocks the inhibition from the AB neuron (being glutamatergic), hence the preburst inhibition is not affected by DA in such conditions. This explains why DA is ineffective in regularizing the spiking of the LP neuron when glutamatergic connections are blocked.

The overall effect of DA on the PD is also complex. On the one hand, it hyperpolarizes the PD (Ayali & Harris-Warrick, 1999) by affecting intrinsic voltage-gated conductances and it also enhances the phasic inhibition by depolarizing the presynaptic LP (Flamm & Harris-Warrick, 1986a) and increasing the graded component of the LP–PD synaptic inhibition (Ayali *et al*., 1998). As a result, the ISI signature of the PD neuron becomes more pronounced with well separated point clusters, a clear sign of increased reliability of burst repetitions. Using the dynamic clamp method in our earlier study we simulated the natural phasic inhibition of the PD neuron by the LP (Szücs *et al*., 2003). We found that the strength and timing of the LP-type inhibition were important factors in shaping the dynamics of intraburst spiking of the PD neuron. Considering the above, the DA-induced enhancement of the LP neuron activity probably plays a role in the DA-induced reshaping of the PD neuron signature. At the same time, when inhibition from LP was blocked by PTX, DA still had an effect on the ISI signature of PD. This suggests that the DA-induced modulation of the intrinsic properties of PD also contributes to the changes in its spike patterns.

The AB neuron is electrically connected to the two PD neurons. The voltage waveforms of the normal bursting PD and AB neurons are remarkably similar and synchronized. However, synchronization is

observed only at the time scale of bursts and the spike times of the AB and PD neurons are virtually uncorrelated. In normal conditions, the AB produces more spikes per burst than the PD. DA depolarizes the AB and hyperpolarizes the PD, therefore resulting in even greater difference between the spike numbers (and frequencies) of the AB and the PD. Subsequently, we believe that the AB plays little if any role in the DA-induced modulation of spike dynamics of the PD neuron. Rather, the level of phasic inhibition (input from the LP) and the intrinsic hyperpolarization are the key factors in shaping the spike dynamics of the PD neuron under the action of DA.

The phasic inhibition preceding the burst of the postsynaptic neuron is a common factor in the regularization of spiking of both the LP and the PD neurons. Although the intrinsic properties and synaptic connectivity of the two types of neurons are different, they both display a similar response to preburst synaptic inhibition: regularization and patterning of the spiking within the burst. This is clearly shown by the clustering of the ISI return maps. As we reported earlier, the evolution (slope) of the membrane potential at the onset of the burst of the PD neuron strongly affects the regularity of spike timing within the burst (Szücs *et al*., 2003). Our current observations with DA reveal a similar mechanism in the LP neuron.

Neuronal signatures: consideration of functional consequences

Our recent observations further support the idea that synaptic inputs have a significant impact on the firing pattern of a bursting neuron during its plateau potential. Because the muscles receive discrete trains of spikes from the neurons, it is important to understand the rules of spike train to muscle activity transformation. While muscles tend to act as low-pass filters of the incoming high-frequency bursts, the degree of their contractions depends on the number and temporal distribution of the spikes within bursts (Morris & Hooper, 1997). Besides, due to the nonlinear nature of the neuromuscular transformation, slight changes in the timing of single spikes in the motoneuron output have a strong impact on the muscle response (Brezina *et al*., 2000; Hooper & Weaver, 2000). Considering these, DA can fine-tune the motor output not only by adjusting the frequencies and phases of bursts but also by regulating the number and timing of intraburst spikes.

The characteristic temporal patterns in bursts (the ISI signatures) might also play an important role in tuning the overall burst pattern of the entire CPG. While direct experimental evidence for pattern (signature)-dependent reshaping of the overall network activity is not yet available, computer model simulations revealed that changes in the ISI signatures of component neurons can indeed change the overall burst patterns of oscillatory CPGs (Latorre *et al*., 2004). These findings, together with our observations on the lobster pyloric neurons, give further support to the idea that short time-scale oscillations such as the spikes effectively modify the output of the neural network on the longer time scale such as that of the bursts.

The synaptic and chemical modulation of fine temporal patterns of bursting neurons, while observed here in a relatively simple motor pattern generating network, might be only a special case of a more general neural mechanism: dynamic regulation of intraburst spike dynamics. Such regulation can play an important role in sensory processing or, in general, temporal coding of presynaptic activity. While neurons with strong bursting properties are also common in mammalian cortical networks their role in sensory processing is not yet clear. However, recent studies performed on different preparations and computational models support the idea that bursting properties are indeed relevant and useful for information transfer and processing (Reinagel *et al*., 1999; Fanselow *et al*., 2001; Balasubramanian & Berry, 2002; Derjean *et al*., 2003; Kepecs & Lisman, 2003; Krahe & Gabbiani, 2004). As we showed for the pyloric neurons, synaptic factors play an important role in shaping their intraburst dynamics. The same can be expected for sensory neurons or interneurons in more complex systems, especially when considering that bursts can, in principle, transfer information more efficiently than single spikes (Reinagel *et al*., 1999; Balasubramanian & Berry, 2002) and given the fact that the time course (envelope) of bursts is highly sensitive to the preceding history of the membrane potential (including PSPs) (Aizenman & Linden, 1999; Fan *et al*., 2000). A recent work on hippocampal interneurons showed that neuronal signatures (cell-specific and behaviour-related firing patterns) are present even in complex brain networks of mammals and *in vivo* (Klausberger *et al*., 2003). This further supports the idea that such neuronal signatures are continuously reshaped by synaptic factors which, in turn, depend on sensory information. In conclusion, the temporal structure of spikes within bursts has to be taken into account to obtain a better understanding of neural oscillations and their role in pattern generation and information processing.

Acknowledgements

Support for this work came from the Office of Naval Research under Grant ONR N00014-00-1-0181, from the National Science Foundation under grant NSF PHY0097134, from the National Institute of Health under grant NIH R01 NS40110–01A2 and from the Hungarian Science Foundation under grant T043162.

Abbreviations

AB, anterior burster (neuron); CPG, central pattern generator; DA, dopamine; IPSP, inhibitory postsynaptic potential; ISI, interspike interval; LP, lateral pyloric (neuron); PD, pyloric dilator (neuron); PTX, picrotoxin; STG, stomatogastric ganglion.

References

Aizenman, C.D. & Linden, D.J. (1999) Regulation of the rebound depolarization and spontaneous firing patterns of deep nuclear neurons in slices of rat cerebellum. *J. Neurophysiol.*, **82**, 1697–1709.

Ayali, A. & Harris-Warrick, R.M. (1998) Interaction of dopamine and cardiac sac modulatory inputs on the pyloric network in the lobster stomatogastric ganglion. *Brain Res.*, **794**, 155–161.

Ayali, A. & Harris-Warrick, R.M. (1999) Monoamine control of the pacemaker kernel and cycle frequency in the lobster pyloric network. *J. Neurosci.*, **19**, 6712–6722.

Ayali, A., Johnson, B.R. & Harris-Warrick, R.M. (1998) Dopamine modulates graded and spike-evoked synaptic inhibition independently at single synapses in pyloric network of lobster. *J. Neurophysiol.*, **79**, 2063–2069.

Balasubramanian, V. & Berry, M.J., 2nd (2002) A test of metabolically efficient coding in the retina. *Network*, **13**, 531–552.

Bidaut, M. (1980) Pharmacological dissection of pyloric network of the lobster stomatogastric ganglion using picrotoxin. *J. Neurophysiol.*, **44**, 1089–1101.

Brezina, V., Orekhova, I.V. & Weiss, K.R. (2000) The neuromuscular transform: the dynamic, nonlinear link between motor neuron firing patterns and muscle contraction in rhythmic behaviors. *J. Neurophysiol.*, **83**, 207–231.

Dekhuijzen, A.J. & Bagust, J. (1996) Analysis of neural bursting: nonrhythmic and rhythmic activity in isolated spinal cord. *J. Neurosci. Meth.*, **67**, 141–147.

Derjean, D., Bertrand, S., Le Masson, G., Landry, M., Morisset, V. & Nagy, F. (2003) Dynamic balance of metabotropic inputs causes dorsal horn neurons to switch functional states. *Nat. Neurosci.*, **6**, 274–281.

Fan, Y.P., Horn, E.M. & Waldrop, T.G. (2000) Biophysical characterization of rat caudal hypothalamic neurons: calcium channel contribution to excitability. *J. Neurophysiol.*, **84**, 2896–2903.

Fanselow, E.E., Sameshima, K., Baccala, L.A. & Nicolelis, M.A. (2001) Thalamic bursting in rats during different awake behavioral states. *Proc. Natl Acad. Sci. USA*, **98**, 15330–15335.

Faure, P., Kaplan, D. & Korn, H. (2000) Synaptic efficacy and the transmission of complex firing patterns between neurons. *J. Neurophysiol.*, **84**, 3010–3025.

Fitzurka, M.A. & Tam, D.C. (1999) A joint interspike interval difference stochastic spike train analysis: detecting local trends in the temporal firing patterns of single neurons. *Biol. Cybern.*, **80**, 309–326.

Flamm, R.E. & Harris-Warrick, R.M. (1986a) Aminergic modulation in lobster stomatogastric ganglion. I. Effects on motor pattern and activity of neurons within the pyloric circuit. *J. Neurophysiol.*, **55**, 847–865.

Flamm, R.E. & Harris-Warrick, R.M. (1986b) Aminergic modulation in lobster stomatogastric ganglion. II. Target neurons of dopamine, octopamine, and serotonin within the pyloric circuit. *J. Neurophysiol.*, **55**, 866–881.

Harris-Warrick, R.M., Johnson, B.R., Peck, J.H., Kloppenburg, P., Ayali, A. & Skarbinski, J. (1998) Distributed effects of dopamine modulation in the crustacean pyloric network. *Ann. NY Acad. Sci.*, **860**, 155–167.

Harris-Warrick, R.M., Nagy, F. & Nusbaum, M.P. (1992) Neuromodulation of stomatogastric networks by identified neurons and transmitters. In Harris-Warrick, R.M., Marder, E., Selverston, A.I. & Moulins, M. (eds), *Dynamic Biologoical Networks: the Stomatogastric Nervous System.* The MIT Press, Cambridge, MA, pp. 87–137.

Hooper, S.L. & Weaver, A.L. (2000) Motor neuron activity is often insufficient to predict motor response. *Curr. Opin. Neurobiol.*, **10**, 676–682.

Johnson, B.R. & Harris-Warrick, R.M. (1997) Amine modulation of glutamate responses from pyloric motor neurons in lobster stomatogastric ganglion. *J. Neurophysiol.*, **78**, 3210–3221.

Johnson, B.R., Kloppenburg, P. & Harris-Warrick, R.M. (2003) Dopamine modulation of calcium currents in pyloric neurons of the lobster stomatogastric ganglion. *J. Neurophysiol.*, **90**, 631–643.

Johnson, B.R., Peck, J.H. & Harris-Warrick, R.M. (1993) Amine modulation of electrical coupling in the pyloric network of the lobster stomatogastric ganglion. *J. Comp. Physiol. [a]*, **172**, 715–732.

Johnson, B.R., Peck, J.H. & Harris-Warrick, R.M. (1995) Distributed amine modulation of graded chemical transmission in the pyloric network of the lobster stomatogastric ganglion. *J. Neurophysiol.*, **74**, 437–452.

Kepecs, A. & Lisman, J. (2003) Information encoding and computation with spikes and bursts. *Network*, **14**, 103–118.

Klausberger, T., Magill, P.J., Marton, L.F., Roberts, J.D., Cobden, P.M., Buzsaki, G. & Somogyi, P. (2003) Brain-state- and cell-type-specific firing of hippocampal interneurons in vivo. *Nature*, **421**, 844–848.

Kloppenburg, P., Levini, R.M. & Harris-Warrick, R.M. (1999) Dopamine modulates two potassium currents and inhibits the intrinsic firing properties of an identified motor neuron in a central pattern generator network. *J. Neurophysiol.*, **81**, 29–38.

Krahe, R. & Gabbiani, F. (2004) Burst firing in sensory systems. *Nat. Rev. Neurosci.*, **5**, 13–23.

Latorre, R., de Borja Rodriguez, F. & Varona, P.P. (2004) Effect of individual spiking activity on rhythm generation of central pattern generators. *Neurocomputing*, **58–60**, 535–540.

Marder, E. & Eisen, J.S. (1984) Transmitter identification of pyloric neurons: electrically coupled neurons use different transmitters. *J. Neurophysiol.*, **51**, 1345–1361.

Morris, L.G. & Hooper, S.L. (1997) Muscle response to changing neuronal input in the lobster (*Panulirus interruptus*) stomatogastric system: spike number- versus spike frequency-dependent domains. *J. Neurosci.*, **17**, 5956–5971.

Mulloney, B. & Selverston, A.I. (1974) Organization of the stomatogastric ganglion in the lobster. I. Neurons driving the lateral teeth. *J. Comp. Physiol.*, **91**, 1–32.

Nagy, F., Cardi, P. & Cournil, I. (1994) A rhythmic modulatory gating system in the stomatogastric nervous system of Homarus gammarus. I. Pyloric-related neurons in the commissural ganglia. *J. Neurophysiol.*, **71**, 2477–2489.

Peck, J.H., Nakanishi, S.T., Yaple, R. & Harris-Warrick, R.M. (2001) Amine modulation of the transient potassium current in identified cells of the lobster stomatogastric ganglion. *J. Neurophysiol.*, **86**, 2957–2965.

Reinagel, P., Godwin, D., Sherman, S.M. & Koch, C. (1999) Encoding of visual information by LGN bursts. *J. Neurophysiol.*, **81**, 2558–2569.

Ruskin, D.N., Bergstrom, D.A., Kaneoke, Y., Patel, B.N., Twery, M.J. & Walters, J.R. (1999) Multisecond oscillations in firing rate in the basal ganglia: robust modulation by dopamine receptor activation and anesthesia. *J. Neurophysiol.*, **81**, 2046–2055.

Russell, D.F. & Hartline, D.K. (1982) Slow active potentials and bursting motor patterns in pyloric network of the lobster, Panulirus interruptus. *J. Neurophysiol.*, **48**, 914–937.

Sanderson, A.C. & Kobler, B. (1976) Sequential interval histogram analysis of non-stationary neuronal spike trains. *Biol. Cybern*, **22**, 61–71.

Segundo, J.P., Sugihara, G., Dixon, P., Stiber, M. & Bersier, L.F. (1998) The spike trains of inhibited pacemaker neurons seen through the magnifying glass of nonlinear analyses. *Neuroscience*, **87**, 741–766.

Svensson, E., Woolley, J., Wikstrom, M. & Grillner, S. (2003) Endogenous dopaminergic modulation of the lamprey spinal locomotor network. *Brain Res.*, **970**, 1–8.

Szücs, A., Pinto, R.D., Rabinovich, M.I., Abarbanel, H.D. & Selverston, A.I. (2003) Synaptic modulation of the interspike interval signatures of bursting pyloric neurons. *J. Neurophysiol.*, **89**, 1363–1377.

Zilberstein, Y., Fuchs, E., Hershtik, L. & Ayali, A. (2004) Neuromodulation for behavior in the locust frontal ganglion. *J. Comp. Physiol. [Neuroethol. Sens. Neural Behav. Physiol.]*, **190**, 301–309.